# Supporting Information

## Selection of Aggregation-caused Quenching-based Fluorescent Tracer for Imaging Studies in Nano Drug Delivery Systems

Xin Ji[a], Yifan Cai[c], Xiaochun Dong[b], Wei Wu[c] and Weili Zhao *[a,b]

[a] Key Laboratory for Special Functional Materials of Ministry of Education, National & Local Joint Engineering Research Center for High-efficiency Display and Lighting Technology, and School of Materials Science and Engineering, Henan University, Kaifeng, 475004, P. R. China.

[b.] Department of Medicinal Chemistry, School of Pharmacy, Fudan University, Shanghai, 201203, P. R. China.

[c.] Key Laboratory of Smart Drug Delivery of MOE, School of Pharmacy, Fudan University, Shanghai 201203, P. R. China.

*Corresponding Authors

E-mail: zhaow@henu.edu.cn

## Table of contents

## Apparatus and reagents

All fluorescent dyes were supplied from Shanghai Energy Biopharma Co., Ltd. (ALA@energy). All reagents were purchased from commercial suppliers and used without further purification. DMSO in chromatographic purity was used in detection. Anhydrous solvents were acquired by standard methods prior to use. TLC analysis was performed on silica gel plates GF254 and chromatography was carried out on 200−300 mesh silica gel (Qingdao Haiyang Chemical, China). ^{1}H NMR spectra were recorded on a Varian Model Mercury 600 MHz spectrometer.^{1}H NMR chemical shifts ($\delta$) are given in ppm (s = singlet, d = doublet, t= triplet, q = quartet, m = multiplet) downfield from $Me_4Si$. ^{13}C NMR spectra were recorded on a Varian Model Mercury 600 MHz spectrometer. Spectrometer UV-vis spectra were acquired on a Lengguang 759S UV-visible spectrophotometer (Lengguang Tech, China). Fluorescence spectra were measured by Lengguang F98 fluorescence spectrophotometer (Lengguang Tech, China). Electrospray ionization (ESI) mass spectra were acquired with Agilent 1100Series LC/MSD and AB SCIEX Triple TOFTM 5600+ mass spectrometer. HRMS (high resolution mass spectrometry, DART positive) spectra were obtained on Thermo Fisher Scientific LTQ FT Ultra. All spectra were recorded at room temperature, except for the confocal laser scanning microscopic images.

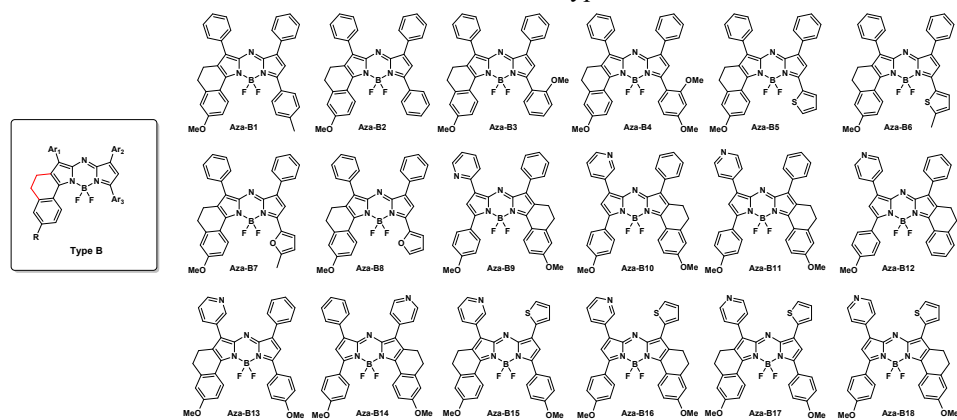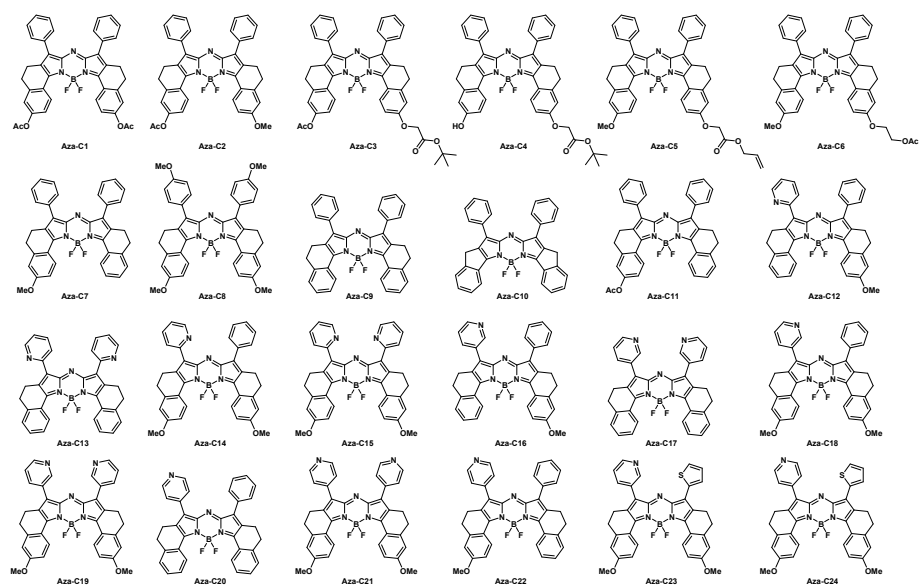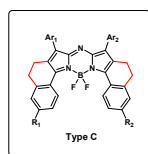# Supplementary schemes
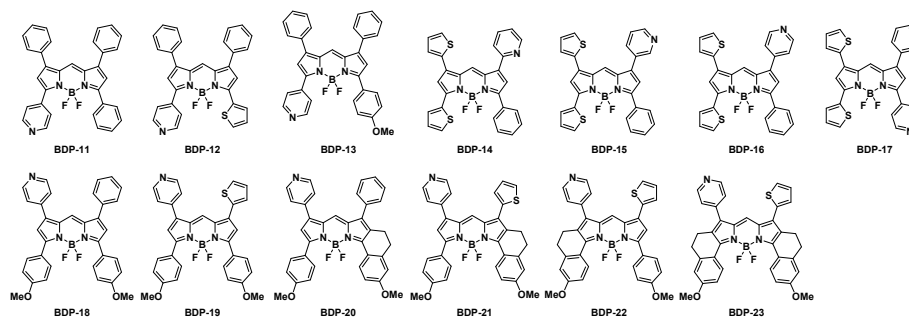


**Scheme S1.** Chemical Structures of BODIPYs.
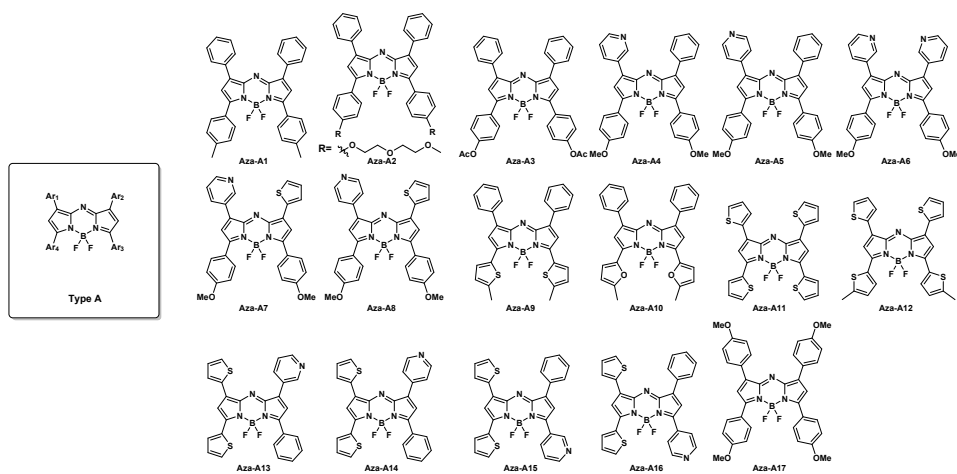


**Scheme S2.** Chemical Structures of Type A Aza-BODIPYs



**Scheme S3.** Chemical Structures of Type B Aza-BODIPYs

**Scheme S4.** Chemical Structures of Type C Aza-BODIPYs

# Supplementary table

**Table S1** Photophysical properties of simple BODIPYs

| Entry | $\lambda_{abs}$ (nm)[a] | $\lambda_{em}$ (nm)[a] | Stokes' shift (nm)[a] | FWHM (nm)[a] | $\varepsilon$ (M$^{-1}$ cm$^{-1}$)[a] | $\Phi$ | $\varepsilon*\Phi$ |
|---|---|---|---|---|---|---|---|
| **BDP-1** | 497 | 507 | 10 | 10 | 79380 | 0.67[b] | 53184 |
| **BDP-2** | 499 | 505 | 6 | 17 | 85600 | 0.92[b] | 78828 |
| **BDP-3** | 647 | 662 | 15 | 30 | 102460 | 0.28[c] | 28688 |
| **BDP-4** | 682 | 697 | 15 | 36 | 72288 | 0.10[d] | 7228 |
| **BDP-5** | 519 | 540 | 21 | 41 | 58860 | 0.32[b] | 18835 |
| **BDP-6** | 561 | 596 | 35 | 49 | 44410 | 0.38[b] | 16876 |
| **BDP-7** | 594 | 613 | 19 | 38 | 59330 | 0.43[b] | 25512 |
| **BDP-8** | 616 | 595 | 21 | 35 | 88900 | 0.40[b] | 35560 |
| **BDP-9** | 631 | 654 | 23 | 41 | 99570 | 0.18[c] | 17923 |
| **BDP-10** | 634 | 659 | 25 | 40 | 138460 | 0.17[c] | 23538 |
| **P2** | 703 | 735 | 32 | 45 | 10500 | 0.35 | 36750 |
| **P4** | 643 | 661 | 18 | 32 | 149100 | 0.65 | 96915 |

[a] Measured in CH$_3$CN.

[b] $\Phi_f$ is the relative fluorescence quantum yield estimated by using **Rhodamine B** ($\Phi_f = 0.65$ in Ethanol) as a fluorescence standard.

[c] $\Phi_f$ is the relative fluorescence quantum yield estimated by using **P4** ($\Phi_f = 0.65$ in CH$_3$CN) as a fluorescence standard.

[d] $\Phi_f$ is the relative fluorescence quantum yield estimated by using **P2** ($\Phi_f = 0.35$ in CH$_3$CN) as a fluorescence standard.

**Table S2** Photophysical properties of the BODIPYs

| Entry | $\lambda_{abs}$ (nm)[a] | $\lambda_{em}$ (nm)[a] | Stokes' shift (nm)[a] | FWHM (nm)[a] | $\varepsilon$ (M$^{-1}$ cm$^{-1}$)[a] | $\Phi$ | $\varepsilon*\Phi$ |
|---|---|---|---|---|---|---|---|
| BDP-11 | 573 | 610 | 37 | 39 | 62000 | 0.67 | 41540 |
| BDP-12 | 589 | 615 | 26 | 32 | 71500 | 0.64 | 45760 |
| BDP-13 | 573 | 610 | 37 | 39 | 65600 | 0.66 | 43296 |
| BDP-14 | 609 | 640 | 31 | 36 | 71500 | 0.65 | 46475 |
| BDP-15 | 600 | 633 | 33 | 37 | 57900 | 0.73 | 42267 |
| BDP-16 | 603 | 636 | 33 | 39 | 57600 | 0.68 | 39168 |
| BDP-17 | 603 | 637 | 34 | 39 | 60300 | 0.50 | 30150 |
| BDP-18 | 603 | 652 | 49 | 48 | 54000 | 0.67 | 36180 |
| BDP-19 | 593 | 641 | 48 | 47 | 62100 | 0.68 | 42228 |
| BDP-20 | 625 | 658 | 33 | 40 | 82500 | 0.71 | 58575 |
| BDP-21 | 626 | 665 | 39 | 44 | 66800 | 0.73 | 48764 |
| BDP-22 | 634 | 668 | 34 | 42 | 79900 | 0.52 | 41548 |
| BDP-23 | 664 | 686 | 22 | 37 | 122400 | 0.37 | 45288 |

[a] Measured in CH$_3$CN.

[b] $\Phi_f$ is the relative fluorescence quantum yield estimated by using **P4** ($\Phi_f$ = 0.65 in CH$_3$CN) as a fluorescence standard.

**Table S3** Photophysical properties of the Type A Aza-BODIPYs

| Entry | $\lambda_{abs}$ (nm)[a] | $\lambda_{em}$ (nm)[a] | Stokes' shift (nm)[a] | FWHM (nm)[a] | $\varepsilon$ (M$^{-1}$ cm$^{-1}$)[a] | $\Phi$ | $\varepsilon*\Phi$ |
|---|---|---|---|---|---|---|---|
| Aza-A1 | 656 | 690 | 34 | 39 | 86100 | 0.22 | 18942 |
| Aza-A2 | 683 | 720 | 37 | 46 | 85000 | 0.24 | 20400 |
| Aza-A3 | 649 | 683 | 34 | 40 | 67000 | 0.13 | 8710 |
| Aza-A4 | 685 | 724 | 39 | 46 | 87500 | 0.24 | 21000 |
| Aza-A5 | 690 | 731 | 41 | 56 | 48800 | 0.24 | 11712 |
| Aza-A6 | 688 | 727 | 39 | 50 | 82000 | 0.26 | 21320 |
| Aza-A7 | 698 | 735 | 37 | 53 | 87500 | 0.21 | 18375 |
| Aza-A8 | 703 | 745 | 42 | 55 | 68900 | 0.12 | 8268 |
| Aza-A9 | 732 | 757 | 25 | 39 | 116800 | 0.22 | 25696 |
| Aza-A10 | 742 | 766 | 24 | 41 | 122200 | 0.13 | 15886 |
| Aza-A11 | 733 | 757 | 24 | 37 | 96200 | 0.12 | 11544 |
| Aza-A12 | 754 | 773 | 19 | 42 | 102500 | 0.11 | 11275 |
| Aza-A13 | 688 | 714 | 26 | 40 | 57200 | 0.21 | 12012 |
| Aza-A14 | 691 | 721 | 30 | 44 | 55700 | 0.21 | 11697 |
| Aza-A15 | 684 | 712 | 28 | 41 | 75300 | 0.25 | 18825 |
| Aza-A16 | 682 | 712 | 30 | 46 | 76100 | 0.18 | 13698 |
| Aza-A17 | 687 | 717 | 30 | 52 | 71900 | 0.28 | 20132 |

[a] Measured in CH$_3$CN.

[b] $\Phi_f$ is the relative fluorescence quantum yield estimated by using **P2** ($\Phi_f = 0.35$ in CH$_3$CN) as a fluorescence standard.

**Table S4** Photophysical properties of the Type B Aza-BODIPYs

| Entry | $\lambda_{abs}$ (nm)[a] | $\lambda_{em}$ (nm)[a] | Stokes' shift (nm)[a] | FWHM (nm)[a] | $\varepsilon$ (M$^{-1}$ cm$^{-1}$)[a] | $\Phi$ | $\varepsilon*\Phi$ |
|---|---|---|---|---|---|---|---|
| Aza-B1 | 688 | 721 | 33 | 39 | 94600 | 0.41 | 38786 |
| Aza-B2 | 681 | 711 | 30 | 39 | 72000 | 0.35 | 25200 |
| Aza-B3 | 714 | 735 | 21 | 35 | 120000 | 0.28 | 33600 |
| Aza-B4 | 698 | 739 | 41 | 53 | 75000 | 0.20 | 15000 |
| Aza-B5 | 718 | 741 | 23 | 40 | 108500 | 0.28 | 30380 |
| Aza-B6 | 730 | 754 | 24 | 40 | 115300 | 0.22 | 25366 |
| Aza-B7 | 736 | 761 | 25 | 40 | 149300 | 0.16 | 23888 |
| Aza-B8 | 721 | 742 | 21 | 41 | 141600 | 0.28 | 39648 |
| Aza-B9 | 711 | 743 | 32 | 47 | 82000 | 0.24 | 19680 |
| Aza-B10 | 704 | 737 | 33 | 46 | 88000 | 0.28 | 24640 |
| Aza-B11 | 709 | 744 | 35 | 49 | 65000 | 0.21 | 13650 |
| Aza-B12 | 699 | 729 | 30 | 42 | 77000 | 0.26 | 20020 |
| Aza-B13 | 714 | 747 | 33 | 47 | 91900 | 0.22 | 20218 |
| Aza-B14 | 713 | 746 | 33 | 48 | 71100 | 0.17 | 12087 |
| Aza-B15 | 719 | 750 | 31 | 44 | 48800 | 0.20 | 9760 |
| Aza-B16 | 716 | 752 | 36 | 49 | 91900 | 0.13 | 11947 |
| Aza-B17 | 724 | 758 | 34 | 45 | 79000 | 0.11 | 8690 |
| Aza-B18 | 720 | 760 | 40 | 48 | 57880 | 0.10 | 5788 |

[a] Measured in $CH_3CN$.

[b] $\Phi_f$ is the relative fluorescence quantum yield estimated by using **P2** ($\Phi_f$ = 0.35 in $CH_3CN$) as a fluorescence standard.

**Table S5** Photophysical properties of the Type C Aza-BODIPYs

| Entry | $\lambda_{abs}$ (nm)[a] | $\lambda_{em}$ (nm)[a] | Stokes' shift (nm)[a] | FWHM (nm)[a] | $\varepsilon$ ($M^{-1}$ $cm^{-1}$)[a] | $\Phi$ | $\varepsilon*\Phi$ |
|---|---|---|---|---|---|---|---|
| **Aza-C1** | 706 | 725 | 19 | 33 | 123000 | 0.27 | 33210 |
| **Aza-C2** | 718 | 739 | 21 | 43 | 115000 | 0.29 | 33350 |
| **Aza-C3** | 718 | 735 | 17 | 42 | 37000 | 0.31 | 11470 |
| **Aza-C4** | 730 | 750 | 20 | 39 | 106000 | 0.20 | 21200 |
| **Aza-C5** | 714 | 732 | 18 | 35 | 112000 | 0.31 | 34720 |
| **Aza-C6** | 715 | 732 | 17 | 35 | 106000 | 0.17 | 18020 |
| **Aza-C7** | 731 | 752 | 21 | 38 | 156000 | 0.24 | 37440 |
| **Aza-C8** | 728 | 748 | 20 | 37 | 153000 | 0.30 | 45900 |
| **Aza-C9** | 699 | 716 | 17 | 31 | 104000 | 0.29 | 30160 |
| **Aza-C10** | 698 | 709 | 11 | 27 | -[c] | -[c] | -[c] |
| **Aza-C11** | 703 | 719 | 16 | 36 | -[c] | -[c] | -[c] |
| **Aza-C12** | 725 | 744 | 19 | 39 | 129000 | 0.23 | 29670 |
| **Aza-C13** | 718 | 740 | 22 | 42 | 122000 | 0.15 | 18300 |
| **Aza-C14** | 744 | 764 | 20 | 39 | 133000 | 0.14 | 18620 |
| **Aza-C15** | 755 | 776 | 21 | 48 | 138000 | 0.10 | 13800 |
| **Aza-C16** | 716 | 735 | 19 | 35 | 139000 | 0.27 | 37530 |
| **Aza-C17** | 704 | 724 | 20 | 31 | 141000 | 0.23 | 32430 |
| **Aza-C18** | 736 | 757 | 21 | 38 | 122000 | 0.21 | 25620 |
| **Aza-C19** | 740 | 760 | 20 | 38 | 138000 | 0.16 | 22080 |
| **Aza-C20** | 706 | 726 | 20 | 33 | 122000 | 0.21 | 25620 |
| **Aza-C21** | 750 | 767 | 17 | 42 | 104000 | 0.09 | 9360 |
| **Aza-C22** | 724 | 744 | 20 | 40 | 106000 | 0.15 | 15900 |
| **Aza-C23** | 748 | 769 | 21 | 40 | 71100 | 0.07 | 4973 |
| **Aza-C24** | 753 | 778 | 25 | 50 | 112300 | 0.04 | 4492 |

[a] Measured in $CH_3CN$.

[b] $\Phi_f$ is the relative fluorescence quantum yield estimated by using **P2** ($\Phi_f = 0.35$ in $CH_3CN$) as a fluorescence standard.

[c] Such data could not be obtained due to the limited solubility of the probes in $CH_3CN$.

**Table S6** Particle size, PDI and zeta potential of fluorescently labeled PMs

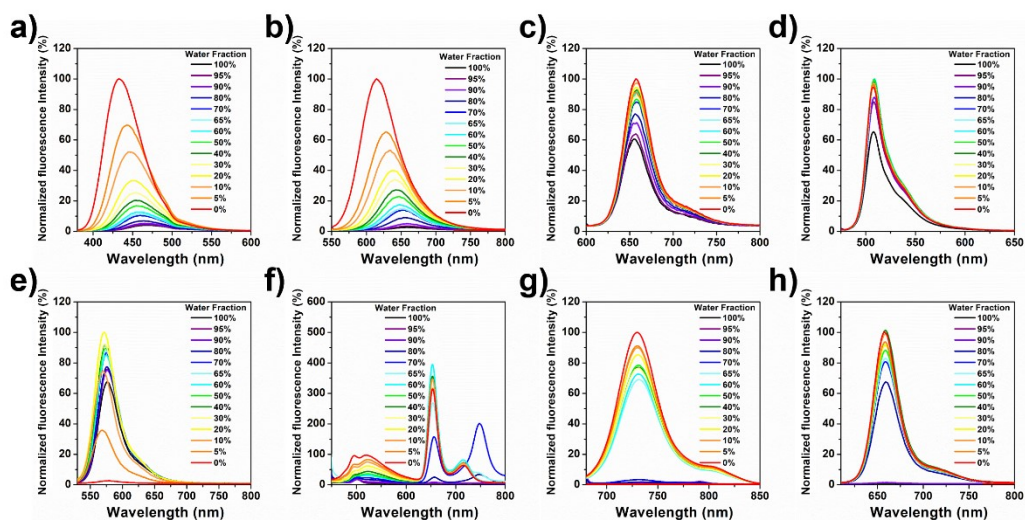| Probe | Size (nm) | PDI | Zeta potential (mV) | EE (%) |
|---|---|---|---|---|
| P2 | 57.19±1.42 | 0.161±0.02 | −7.97±0.25 | 97.2 |
| Aza-C7 | 52.73±0.15 | 0.175±0.01 | −6.80±0.41 | 95.6 |
| DiR | 55.81±0.82 | 0.176±0.02 | −6.59±0.20 | 98.9 |

# Supplementary data



**Figure S1** Fluorescence spectra (normalized) of the probes (250 nM) in acetonitrile/water systems as a function of water fractions. (a) For **7D4MC**, excitation at 365 nm; (b) for **Nile Red**, excitation at 535 nm; (c) for **Cy5 DIME**, excitation at 580 nm; (d) for **TMBDY**, excitation at 460 nm; (e) for **Rhodamine B**, excitation at 510 nm; (f) for **TPP**, excitation at 460 nm; (g) for **P2**, excitation at 680 nm; (h) for **P4**, excitation at 600 nm (slit: 2/5 nm).
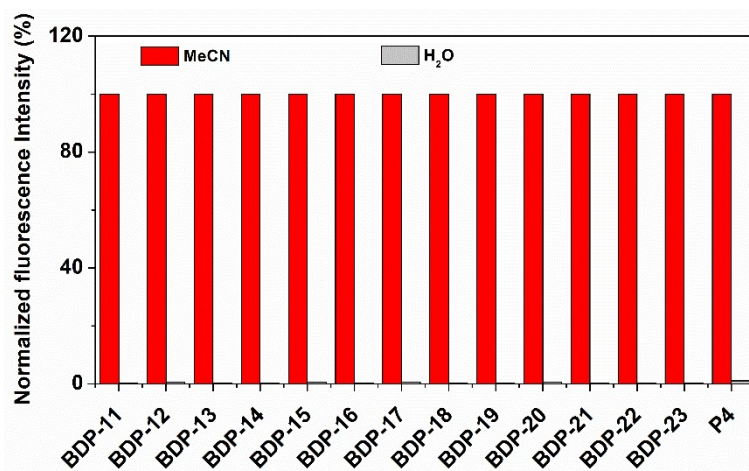


**Figure S2** Normalized fluorescence intensity (%) change of the probes (250 nmol/L) in acetonitrile and water. For ease of comparison, fluorescence intensity is displayed as percentages of the fluorescence intensity of probe-acetonitrile solution with the same volume. The excitation was set at the wavelength blue-shifted by 20 nm compared to the maximal absorption wavelength of the probe (slit: 5/5 nm).
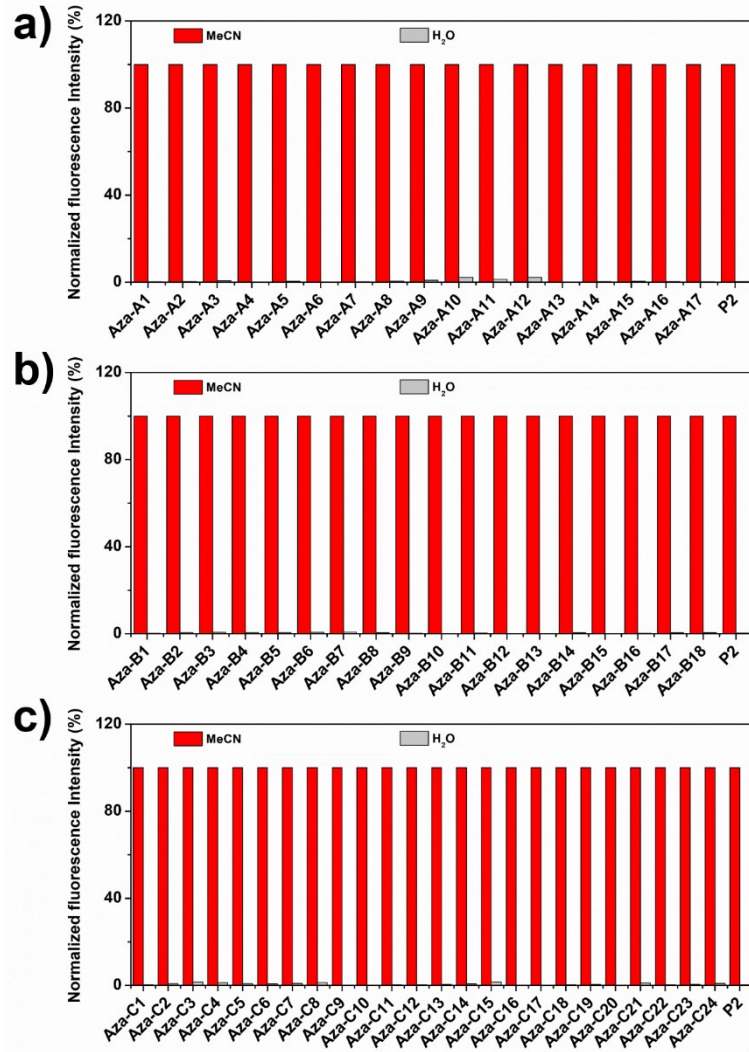
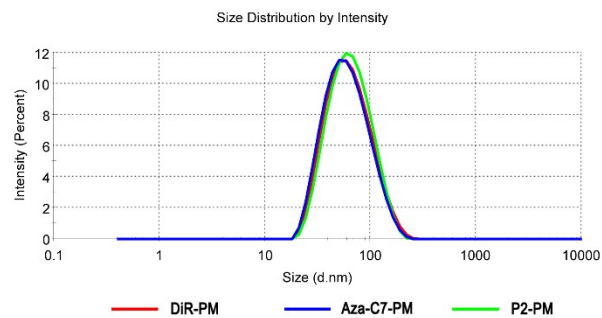**Figure S3** Normalized fluorescence of the probes (250 nmol/L, a: **Type A** Aza-BODIPY; b: **Type B** Aza-BODIPY; c: **Type C** Aza-BODIPY) in water relative to acetonitrile. The excitation was set at the wavelength blue-shifted by 20 nm compared to the maximal absorption wavelength of the probe (slit: 5/5 nm).



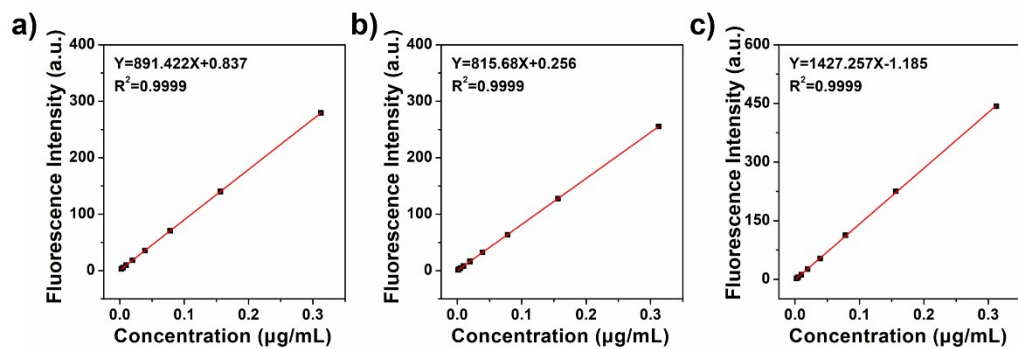**Figure S4.** Particle size distribution for fluorescently labeled PMs.

**Figure S5.** The standard curves of probes (a: **P2**, b: **Aza-C7** and c: **DiR**) in DMSO.
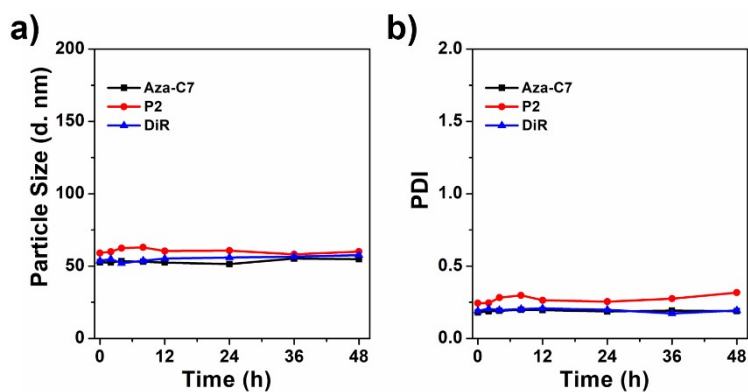


**Figure S6.** Particle size and PDI stability in water for fluorescently labeled PMs.